Geochemistry, Geophysics, Geosystems

RESEARCH ARTICLE
10.1029/2021GC009700

Special Section:
Tethyan dynamics: from rifting to collision

Mantle Flow Patterns Beneath the Junction of Multiple Subduction Systems Between the Pacific and Tethys Domains, SE Asia: Constraints From *SKS*-Wave Splitting Measurements

Lingmin Cao[1,2], Xiaobo He[3], Liang Zhao[4,5], ChuanChuan Lü[6], Tianyao Hao[5,7,8], Minghui Zhao[1,2,5], and Xuelin Qiu[1,2,5]

[1]Key Laboratory of Ocean and Marginal Sea Geology, South China Sea Institute of Oceanology, Chinese Academy of Sciences, Guangzhou, China, [2]Southern Marine Science and Engineering Guangdong Laboratory (Guangzhou), Guangzhou, China, [3]Department of Marine Sciences, Zhejiang Ocean University, Zhoushan, China, [4]State Key Laboratory of Lithospheric Evolution, Institute of Geology and Geophysics, Chinese Academy of Sciences, Beijing, China, [5]University of Chinese Academy of Sciences, Beijing, China, [6]Department of Earth Sciences, Bullard Laboratories, University of Cambridge, Cambridge, UK, [7]Key Laboratory of Petroleum Resources Research, Institute of Geology and Geophysics, Chinese Academy of Sciences, Beijing, China, [8]Key Laboratory of Submarine Geosciences, State Oceanic Administration, Hangzhou, China

Key Points:

- Seismic anisotropy in the multiple subduction zones around the Celebes Sea is characterized by *SKS* splitting analyses
- The Sangihe slab edges likely deflect the surrounding flow
- A large mantle wedge flow induced by the subduction of the Sangihe slab broadly influences the regional upper mantle dynamics

Correspondence to:
L. Cao and X. He,
cao_lingmin@126.com;
xiaobo.he@zjou.edu.cn

Citation:
Cao, L., He, X., Zhao, L., Lü, C., Hao, T., Zhao, M., & Qiu, X. (2021). Mantle flow patterns beneath the junction of multiple subduction systems between the Pacific and Tethys domains, SE Asia: Constraints from *SKS*-wave splitting measurements. *Geochemistry, Geophysics, Geosystems*, *22*, e2021GC009700. https://doi.org/10.1029/2021GC009700

Received 8 FEB 2021
Accepted 13 AUG 2021

Abstract The region around the Celebes Sea, SE Asia, is evolving within a convergent tectonic environment involving the Pacific plate to the east and the Indian-Australian plate to the south. It is arguably one of the most tectonically complex regions in the world and serves as an ideal setting to study dynamic interactions between the Pacific and Tethys tectonic domains. The issue of which subducting plate plays a leading role in governing the regional mantle flow is not well understood. Mantle flow can be characterized by seismic anisotropy observations, providing clues for understanding regional tectonics. We conducted *SKS*-wave splitting analysis by using data from seven seismic stations located around the Celebes Sea. Our results, when combined with previous observations, suggest the presence of various types of mantle flow in this area, including (a) corner flow in the mantle wedge above the westward-subducting Molucca Sea (Sangihe) slab, (b) two-layer anisotropy related to the eastward-subducting Molucca Sea (Halmahera) slab, (c) deflected flow due to proximity to the Sangihe slab's edges, (d) trench-normal mantle flow beneath southeastern Borneo due to the subduction of the Indian-Australian plate, and (e) Northwest Borneo-Palawan trough-parallel mantle flow beneath northeastern Borneo. Various types of mantle flow indicate that the dynamic interactions of adjacent subduction zones played crucial roles in influencing the regional upper mantle dynamics between the Tethys and western Pacific domains since the breakup of the Gondwana supercontinent in the Mesozoic.

1. Introduction

The term "poly-island ocean" is widely used to describe the Paleo-Tethys tectonic and geographical pattern (Fang, 2002; B. P. Liu et al., 1991). Among the present vast oceans, the Indonesian Archipelago serves as one of the most typical examples of "poly-island oceans" due to its unique geologic features. Specifically, it connects with the open western Pacific to the east and the hinterland of subduction and collision between the Indian-Australian and Eurasian plates to the west. The latter regime inherits the main characteristics of Tethys tectonics related to the northward subduction of the Indian-Australian plate.

The Celebes Sea lies to the east of the Indonesian Archipelago. It is an ideal research area to study dynamic interactions between multiple microcontinents and oceans in a "poly-island ocean" domain, owing to its unique geologic location at the junction point of three major tectonic plates: the Indian-Australian, Philippine Sea, and Eurasian plates. In addition, the northeastern, eastern, and southern edges of the Celebes Sea are bordered with several subduction zones, including the Cotabato and North Sulawesi subduction zones and the double-sided subduction of the Molucca Sea plate (Figure 1). Numerical simulations have suggested that dynamic interactions take place in an active, complex tectonic setting composed of multiple

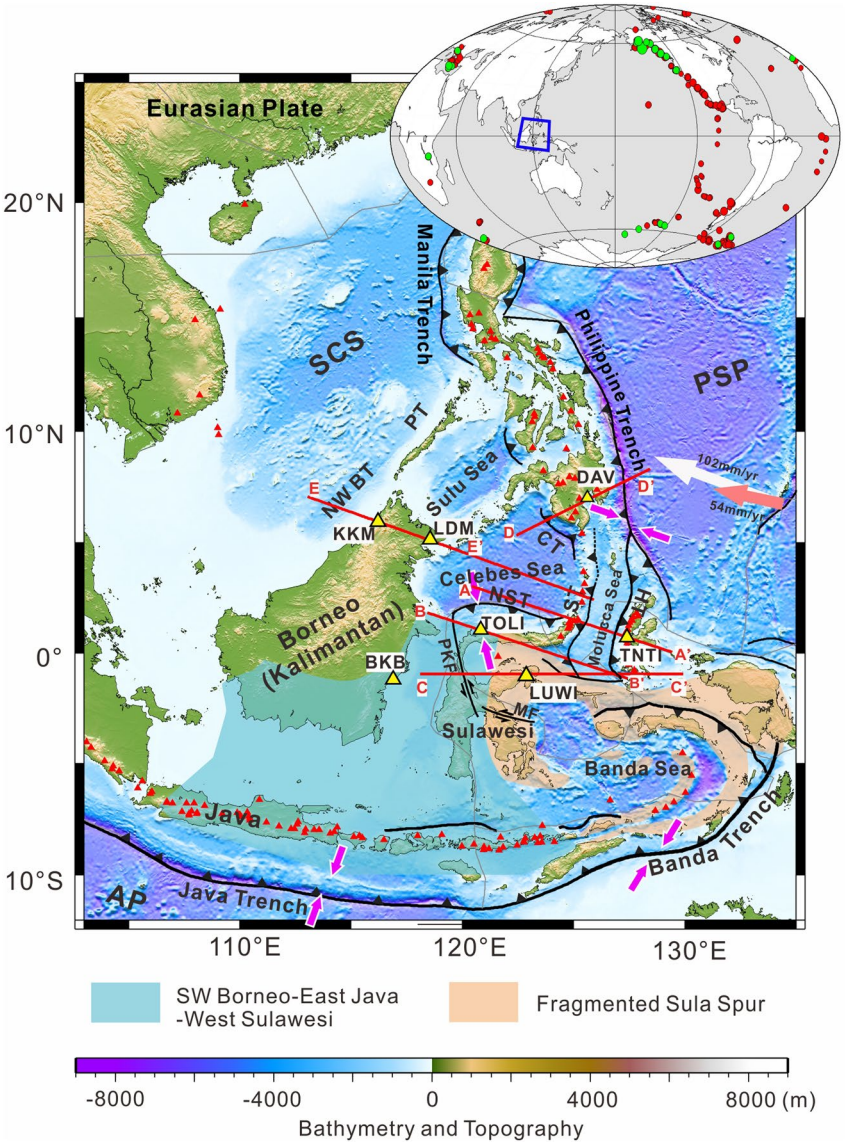

Figure 1. Bathymetric and topographic map showing the locations of the seven broadband seismic stations used in this study and the tectonics of the study area. Yellow triangles mark the seismic stations. Solid red triangles denote Quaternary volcanoes. The black sawtooth lines show the trench location. Translucent shaded regions indicate the ranges of two areas whose crust probably originated from Australian continental fragments and extension by rollback of the Banda slab (modified from R. Hall & Sevastjanova, 2012). Arrows indicate plate motion directions from two different absolute plate motion models (hotspot model (white): Gripp & Gordon, 2002; no-net-rotation model (pink): DeMets et al., 1994). Pink arrow pairs indicate convergence directions between plates or micro-plates on both sides of the trenches (Argus et al., 2011; Bird, 2003; Lallemand et al., 1998; C. Liu & Shi, 2021). Red lines denote the locations of velocity perturbation cross sections, which are further discussed in Figure 7. The scale for the bathymetry and topography is shown at the bottom. AP, Australian Plate; CT, Cotabato Trench; HT, Halmahera Trench; MF, Matano Fault; NST, North Sulawesi Trench; NW BT, Northwest Borneo Trough; PKF, Palu Koro Fault; PSP, Philippine Sea Plate; PT, Palawan Trough; SCS, South China Sea; ST, Sangihe Trench. In the inset, red circles show $M_w > 6.0$ teleseismic events with epicentral distances ranging from 85° to 135° occurring between 2009 and 2019. Green circles show the locations of 26 teleseismic events used in the final analysis. The blue quadrilateral shows the location of the study area.

subducting slabs (e.g., Király et al., 2016, 2018; Lyu et al., 2019; X. Wang et al., 2019). The upper mantle around the Celebes Sea is also proposed to have experienced a complex deformation history due to the subduction of multiple slabs in adjacent subduction zones (e.g., Di Leo et al., 2012a, 2012b; Király et al., 2018; Roy et al., 2017).

The mantle flow system can be characterized by seismic anisotropy. Seismic anisotropy is a physical phenomenon in which seismic waves migrate with varying velocities in different polarization directions. Such anisotropy in the upper mantle is generally considered to be caused mainly by the crystallographic preferred orientation (CPO) of mantle minerals, that is, primarily olivine in the upper mantle, resulting from ductile deformation induced by mantle flow (Christensen, 1984; Hess, 1964; Nicolas & Christensen, 1987; S. Zhang & Karato, 1995). Hence, measurements of seismic anisotropy provide the best tool available to directly explore the flow patterns in the upper mantle.

Our understanding of anisotropic characteristics in the study region benefits from previous measurements by using local *S*, direct *S*, and *SKS*-phase splitting. A series of mantle flow patterns have been revealed, such as toroidal flow around the Celebes Sea slab and subslab mantle flow parallel to the trench beneath the Molucca Sea (Di Leo et al., 2012a, 2012b). Fan and Zhao (2019) conducted 3-D *P* wave anisotropic tomography, which primarily focused on the Philippines to the north of this study area. The analysis of source-side *sS* splitting also plays a role in probing mantle wedge anisotropy, but it is mainly associated with the subduction of the Indian-Australian plate along with the South China Sea and Philippine Sea plates (L. Wang & He, 2020). Despite various efforts around the Celebes Sea and the Molucca Sea, our knowledge of the upper mantle anisotropy is still limited due to the poor spatial coverage of seismic stations.

In this study, to better understand the deformation characteristics in the complex tectonic region, we show upper mantle anisotropic fabrics constrained by measuring teleseismic *SKS*-wave splitting from new seismic data collected from seven broadband stations, six of which have been deployed for long-term observation (>12 years). Also, previous shear-wave splitting measurements (Di Leo et al., 2012a, 2012b; Roy et al., 2017; L. Wang & He, 2020) and a *Vp* velocity model UU-P07 by Amaru (2007) are combined to shed light on the regional upper mantle flow patterns at the corner between the Pacific and Tethys domains.

2. Tectonic Setting

The eastern Indonesian Archipelago, SE Asia, is bordered by tectonically active zones characterized by earthquakes and volcanic activities. Relative to SE Asia, the Eurasian plate is currently moving very slowly (~1 cm/y), whereas the Indian-Australian and Pacific plates are moving toward SE Asia at faster rates (~7 cm/y) (Bird, 2003; Bock et al., 2003; DeMets et al., 2010; Simons et al., 2007). Therefore, the tectonics of the Indonesian Archipelago record the history of long-term subduction and collision caused by these convergent motions during the last 180 Myr (e.g., Wan et al., 2019).

In the study area, southwestern Borneo, East Java, and western and northwestern Sulawesi have been considered as Australian continental fragments that accreted to Sundaland in the Cretaceous (e.g., Parkinson et al., 1998; van Leeuwen et al., 2007; Wakita et al., 1996) (Figure 1). The fragmented Sula Spur southeast of the Celebes Sea (Figure 1), as represented in tectonic reconstructions by R. Hall (1996), is considered to have resulted from extensional fragmentation of the former Sula Spur due to rollback of the subducting Banda slab between ~23 and 2 Ma (R. Hall, 2017). The collision and subduction zones between these microcontinents and oceanic plates in the eastern Indonesian Archipelago offer an opportunity to characterize the convergence process and improve our understanding of oceanic closure and plate collisions, which may shed light on similar events that occurred in the Tethys region.

At present, the area centered on the Celebes Sea plate is wedged between the Indian-Australian, Eurasian, and Philippine Sea plates and encompasses several active subduction zones. A unique feature of the area is double-sided subduction of the Molucca Sea plate; the western part (hereafter called the Sangihe slab) is the oldest active subduction zone along the Indonesia-Philippine Sea plate boundary, where subduction at the Sangihe trench initiated ~25 Ma (Jaffe et al., 2004). The subducting slab reaches a depth of ~650 km with dips of 55–65° in the upper mantle (Cardwell et al., 1980; Tatsumi et al., 1991). The eastern part of the Molucca Sea slab (hereafter called the Halmahera slab) is subducting eastward beneath the Philippine Sea plate at the Halmahera trench to depths of ~200–300 km with shallow dips of 40–45° in the upper mantle (Cardwell et al., 1980; Tatsumi et al., 1991). Subduction initiated ~7 or 10 Ma (Elburg & Foden, 1998; R. Hall & Spakman, 2015). The two magmatic arcs produced by the double-sided subduction of the Molucca Sea plate are currently converging at an average rate of 3–4 cm/yr (Lallemand et al., 1998), and consequent

Table 1
List of Broadband Seismic Stations Used in This Study

Station	Network	Longitude	Latitude	Operation period
BKB	GEOFON	116.90	−1.11	June 2009–(Operating)
TOLI	GEOFON	120.79	1.12	June 2008–July 2012
LUWI	GEOFON	122.77	−1.04	March 2008–(Operating)
TNTI	GEOFON	127.37	0.77	January 2007–(Operating)
DAV	IU	125.58	7.07	December 1994–(Operating)
KKM	MY	116.21	6.04	February 2005–(Operating)
LDM	MY	118.50	5.18	March 2006–(Operating)

arc-arc collision might thus occur at present according to geophysical and geochemical data (Elburg & Foden, 1998; R. Hall & Wilson, 2000; Jaffe et al., 2004; E. A. Silver & Moore, 1978). This raises the question of whether similar anisotropic fabrics can be developed in these two subduction systems that have different dip angles and subducted slab lengths.

South of the Celebes Sea, the slab itself is subducting southward beneath Sulawesi Island along the North Sulawesi trench (e.g., Kopp et al., 1999). Subduction commenced at ∼5 Ma (R. Hall & Spakman, 2015). Seismic evidence suggests that the slab reaches a depth of ∼250 km and collides with the Sangihe slab at a depth of ∼200 km (Cottam et al., 2011; R. Hall & Spakman, 2015; Kopp et al., 1999). Which plate subduction plays a more important role in the upper mantle deformation, however, is not yet well understood.

At the northern edge of the Sangihe plate, the Celebes Sea slab is subducting to a depth of ∼100 km beneath the Philippines at the Cotabato trench (Cardwell et al., 1980), and it subducted at ∼18 Ma (Sajona et al., 1997). Comparing to the subduction of the Celebes Sea slab, the Philippine Sea plate is subducting in an opposite direction to a depth of more than 300 km beneath the Philippines at the Philippine trench, which started subduction at ∼4–5 Ma (Aurelio, 1992; Fan et al., 2017). This region is evolving with the dynamic interactions of multiple subducting slabs.

Farther south, the Indian-Australian slab has been subducting to depths up to 1,200 km in the Java subduction zone but is flat-lying above the 660-km discontinuity in the Banda subduction zone (R. Hall, 2012). Deeper subduction of the Java slab have induced large-scale upper mantle deformation according to anisotropy analysis of source-side *sS*-wave splitting along these subduction zones (L. Wang & He, 2020). However, to what extent its influence on the regional mantle dynamics is still enigmatic.

West of the Celebes Sea saw the onset of subduction of the Proto-South China Sea slab in northern Borneo in the mid-Eocene (∼45 Ma) (Hutchinson, 2006). Subduction lasted until the early Miocene (∼20 Ma) (R. Hall et al., 2008). The fossil Proto-South China Sea slab has been revealed as dipping high-velocity structures in tomographic images (e.g., Amaru, 2007; Fan et al., 2017).

3. Data and Analysis

In this study, we collected seismic data from seven long-operating broadband seismic stations, which are available at the Data Management Center of the Incorporated Research Institutions for Seismology (Table 1). These stations are distributed from Mindanao Island and Halmahera Island in the east to Kalimantan Island in the west (Figure 1). We carefully analyzed 10 years (2009–2019) of recordings from three stations in Kalimantan (BKB, KKM, and LDM), two stations in Sulawesi (TOLI and LUWI) and one station on Halmahera Island (TNTI) and 12 years (2000–2012) of data for DAV in the southern Philippines.

We selected $M_w > 6.0$ earthquakes with epicentral distances ranging from 85° to 135° so that *SKS* incidence angles were less than 15°, avoiding any phase shift due to conversion at the surface (Nuttli, 1961). As a result, 431 *SKS* waveforms at seven stations were used for splitting analysis. The event information was obtained from the International Seismic Center (ISC) Engdahl-van der Hilst-Buland catalog (Engdahl et al., 2020) and the ISC bulletin (Engdahl & Gunst, 1966).

A shear wave usually splits into two orthogonally polarized shear waves when traveling through an anisotropic medium. Two splitting parameters, that is, the fast wave polarization direction (φ) and the delay time (δt) between the fast and slow waves are commonly used to characterize seismic anisotropy. We used the multiple frequency automatic splitting technique software package (Savage et al., 2010; Teanby et al., 2004; A. Wessel, 2010) to determine φ and δt. Before analysis, we bandpass filtered the original waveforms at 0.02–0.2 Hz to enhance the teleseismic *SKS* arrivals. After the splitting correction, in general, anisotropy measurements are considered to be well constrained if they have the following characteristics: (a) good correlation between the fast and slow waveforms, (b) significant amplitude on the radial component of the *SKS* phase, (c) good linearization of particle motion, and (d) a small 95% confidence region. Figure 2 shows a representative example of our splitting measurements (Figure 2a). After correcting for the anisotropic effect, the signal from the transverse component vanishes significantly (Figure 2b), and linearized particle motion is also observed (Figure 2d). Note that a null result can also happen when the shear wave travels in an isotropic medium or the initial polarization (back-azimuth for *SKS*) coincides with the fast or slow polarization direction; in the case of null measurements, no *SKS* energy is observed on the transverse component. A null measurement example is shown in Figure 3. Following the criterions described above, our analysis yielded a total of 18 good splitting measurements and 17 null measurements from a total of 26 teleseismic events (Tables 2 and 3; Figure 1). Most events used in the final analysis occurred in the subduction zones of the East Pacific Rim and the oceanic ridges in the Southwest Indian Ocean and the South Pacific Ocean (Figure 1). Only 8% of the whole data set give reliable results, primarily due to the poor data quality of stations deployed on the islands (Di Leo et al., 2012b; Hammond et al., 2010; Xue et al., 2013); however, all the valid measurements are of good quality.

4. Results

The results measured at the seven stations are summarized in Figures 4 and 5 and Tables 2 and 3. All the analyzed stations exhibit both null and non-null results. Although null results cannot directly provide constraints on splitting times, the initial polarization, which for *SKS* waves usually corresponds to the back-azimuth, simply reflects the estimated fast or slow axis of the anisotropic medium. Therefore, the null results are also informative and can offer additional constraints on the anisotropic structure.

Recordings from station DAV in the southern Philippines yield only one reliable *SKS* splitting measurement with φ of $42 \pm 6.25°$ and δt of 1.44 ± 0.05 s and three null results. Back-azimuths for null results are nearly consistent with the fast direction of the splitting result, which encourage us to draw a conclusion of a simple anisotropic structure in the upper mantle at DAV although the number of events is small. The NE-trending fast direction is perpendicular to the Cotabato trench and oblique to the Philippine and Sangihe trenches. Station TNTI on Halmahera Island also gives only one *SKS* splitting result and four null results. The values of φ and δt at this station are $-55 \pm 3°$ and 1.69 ± 0.09 s, respectively. The fast orientation is oblique to both the subduction direction of the Halmahera slab and the Halmahera trench (Figure 4). It appears to be inconsistent with the back-azimuths of null results, probably indicating a more complex anisotropic structure in the upper mantle at TNTI.

On Sulawesi, TOLI has two splitting and one null results, and LUWI has eight splitting and four null results. The average splitting parameter values are $\varphi = -44°$ and $\delta t = 1.25$ s at TOLI and $\varphi = -74.88°$ and $\delta t = 1.50$ s at LUWI. Events for the results at LUWI cover a good back-azimuth of raypaths between events and this station (shown on an equal-area projection of the splitting parameters at LUWI in Figure 4). No back-azimuthal variation in φ indicates that there is one dominant horizontal layer of anisotropy (P. G. Silver & Savage, 1994). Back-azimuths for null results at the two stations (TOLI and LUWI) are either parallel or normal to the predominant fast directions, further indicating the reliability in the splitting measurements and the presence of a simple anisotropic structure of the upper mantle. Previous *SKS*-phase splitting studies (Di Leo et al., 2012a, 2012b; Figure 6) have also suggested that there is simple one layer of anisotropy beneath both stations LUWI and TOLI.

Three stations BKB, KKM, and LDM in Kalimantan yield six *SKS* splitting measurements: three for BKB, two for KKM, and one for LDM, along with five null results: three for BKB, one for KKM, and one for LDM. The values of δt vary between 0.91 and 2.00 s. The averages of δt at BKB and KKM are 1.35 and 1.70 s, respectively, and δt of 1.69 s occurs at LDM. The fast directions at KKM, LDM, and BKB exhibit NE–SW, WNW–

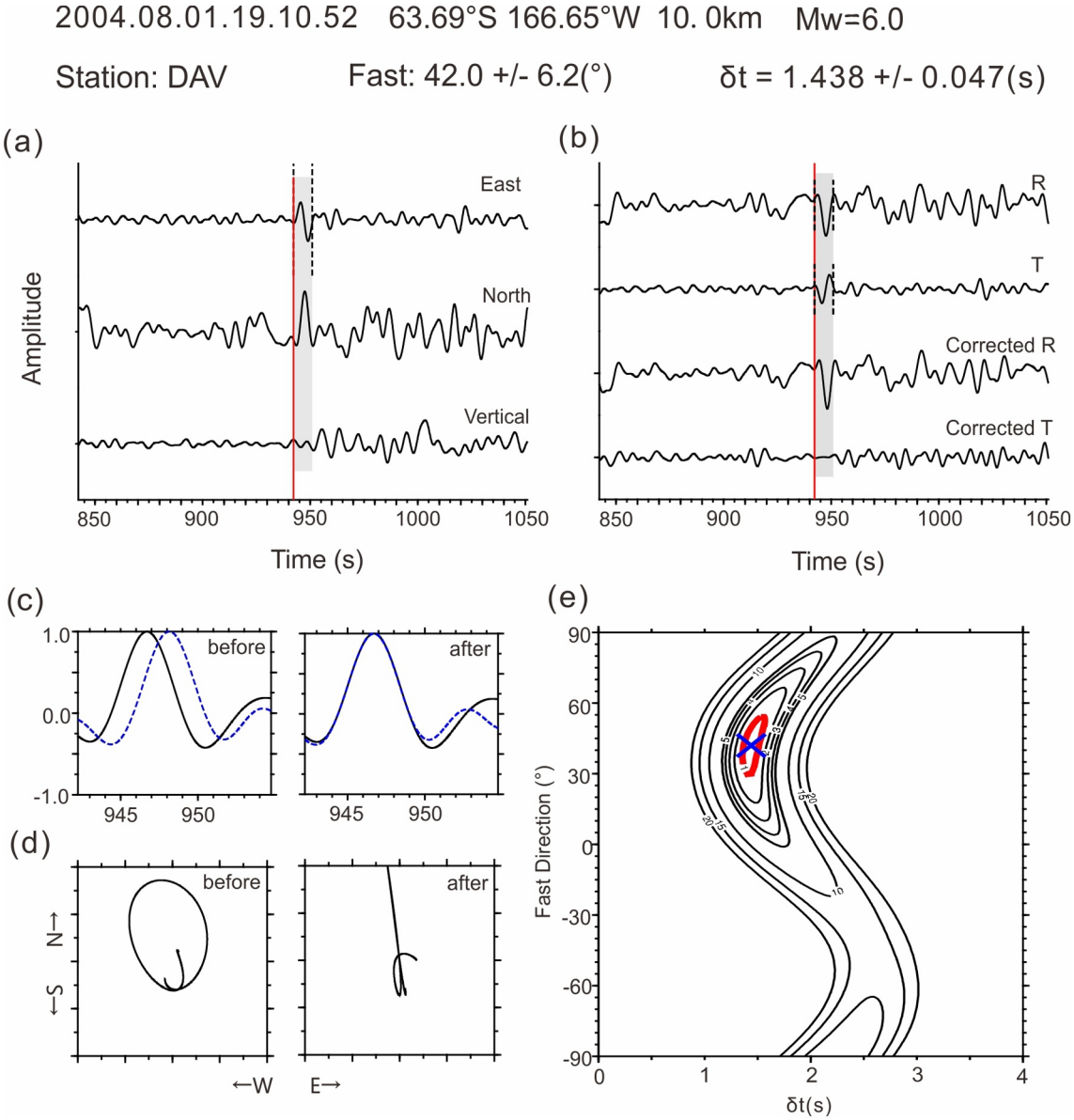

Figure 2. An example of good *SKS*-wave splitting measurements using the multiple frequency automatic splitting technique software package (Savage et al., 2010) at station DAV in the southern Philippines. Event information and splitting parameters are shown at the top. (a) Three components of *SKS* waveforms filtered at 0.02–0.2 Hz; (b) radial (R) and transverse (T) components before and after the splitting correction; (c) normalized fast (solid lines) and slow (dashed lines) shear-wave waveforms before and after the splitting correction; (d) normalized particle motion; (e) results of a grid search for the optimal φ and δt (cross) with the thick red contour indicating the 95% confidence interval. In panels (a and b), vertical long lines mark the arrival of the *SKS* phase, which are manually picked. The two dashed lines mark the time windows for splitting measurements.

ESE, and N–S trends, respectively, while back-azimuths for null results are either sub-parallel or subnormal to the observed fast directions. No notable back-azimuthal dependence of φ is observed, thus indicating one dominant horizontal layer of anisotropy in the upper mantle beneath each station.

5. Discussion

5.1. Mantle Flow Systems in a Subduction Zone

In most subduction zones, seismic anisotropy in the upper mantle is caused mainly by the CPO of olivine, which is induced by mantle flow controlled by slab subduction (Wolfe & Silver, 1998). It is often attributed

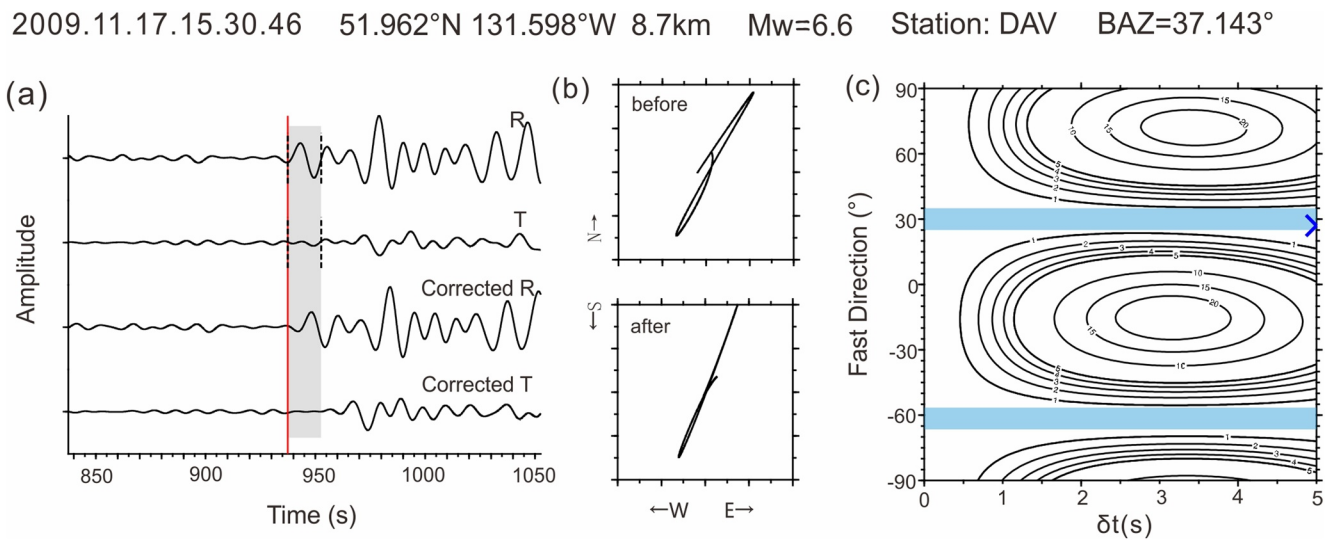

Figure 3. An example of a null result at station DAV. Event information is shown at the top. (a) Radial (R) and transverse (T) components before and after the splitting correction; (b) normalized particle motion before and after the splitting correction; (c) the contour plot of the tangential energy in 2D searching, where the two belts marked in transparent blue indicate the two possible fast directions constrained by the null results.

to two dominant regions, including the mantle wedge above the slab and the subslab mantle below the subducting slab (C. E. Hall et al., 2000; Ribe, 1989). In addition, the overriding plate and subducting slab itself may contribute to the anisotropy (Long, 2013). In general, corner flow in the mantle wedge is developed by viscous coupling between the down-going slab and the overlying mantle, leading to a trench-normal fast-ax-

Table 2
Event Information and SKS-Phase Splitting Measurements

Station	No.	Origin time	Longitude (°E)	Latitude (°N)	Depth (km)	M_W	BAZ	δt (s)	$\sigma_{\delta t}$ (s)	ϕ (°)	σ_ϕ (°)
BKB	1	2013.1012.131153	23.37	35.53	46.9	6.4	305.35	2.00	0.16	18	8.25
	2	2016.1030.064019	13.10	42.83	9.6	6.1	313.33	0.91	0.11	0	7
	3	2018.0128.160303	9.68	−53.06	10	6.6	215.76	1.16	0.07	−8	5.5
DAV	1	2004.0801.190309	−166.65	−63.69	10	6	155.59	1.44	0.05	42	6.25
KKM	1	2011.0401.132911	26.55	35.73	75.5	6.1	305.38	1.84	0.38	62	18
	2	2013.0105.085819	−134.80	55.23	3.1	6.5	32.98	1.56	0.40	55	14.75
LDM	1	2011.0401.132911	26.55	35.73	75.5	6.1	305.57	1.69	0.14	−77	3.5
LUWI	1	2009.1206.173637	33.82	−10.16	15	6	259.93	1.53	0.14	83	3.25
	2	2009.1208.030857	33.82	−9.98	10.4	6	260.10	1.5	0.078	81	1.5
	3	2009.1219.231917	33.83	−10.02	14	6	260.07	1.94	1.25	−87	45.25
	4	2010.0411.220811	−3.48	37.01	619.6	6	312.46	1.44	0.07	−76	6
	5	2011.1102.145928	−128.92	−55.11	10	6.1	146.41	1.00	1.22	−42	28.75
	6	2012.1030.024901	−132.11	52.15	9.5	6.1	37.17	1.84	0.06	−51	1.25
	7	2015.0729.023558	−153.33	59.97	121.2	6.2	30.03	1.13	0.14	−75	2.75
	8	2018.1130.172929	−149.96	61.35	46.7	7	28.78	1.56	0.05	−71	1.25
TNTI	1	2009.1208.030857	33.82	−9.98	10.4	6	260.11	1.69	0.09	55	3
TOLI	1	2009.1208.030857	33.82	−9.98	10.4	6	260.01	0.78	0.13	−31	7
	2	2010.0411.220811	−3.48	37.01	619.6	6.3	312.59	1.72	0.20	−57	5.5

Note. $\sigma_{\delta t}$ and σ_ϕ are the standard deviations of δt and ϕ, respectively.

Table 3
Event Information and SKS-Phase Null Measurements

Station	No.	Origin time	Longitude (°E)	Latitude (°N)	Depth (km)	M_W	BAZ
BKB	1	2014.0424.031011	−127.652	49.6483	9.8	6	37.8835
	2	2018.0123.093142	−149.073	56.0464	25	7.9	34.0957
	3	2018.1130.172929	−149.955	61.3464	46.7	7	28.7979
DAV	1	2007.0120.062105	−29.4544	−55.321	10	6.2	197.808
	2	2009.1117.153046	−131.598	51.9622	8.7	6.6	37.143
	3	2010.0110.002741	−124.467	40.6654	20.6	6.5	46.6073
KKM	1	2009.0416.145706	−27.0291	−60.2882	17.6	6	199.965
LDM	1	2018.1130.172929	−149.955	61.3464	46.7	7	28.8724
LUWI	1	2009.1231.092324	−150.805	−59.6401	10	6	149.5
	2	2014.0310.051813	−125.087	40.7235	6.1	6.3	47.5208
	3	2014.0717.114934	−140.423	60.3186	3.2	6	29.707
	4	2018.1115.230901	−122.044	−56.2363	10	6.3	148.783
TNTI	1	2013.0616.213906	25.1864	34.4242	25	6.1	304.963
	2	2013.1012.131153	23.3718	35.5277	46.9	6.4	306.286
	3	2014.0604.115858	−136.779	59.0281	12.9	6	30.9909
	4	2014.0717.114934	−140.423	60.3186	3.2	6	29.8237
TOLI	1	2009.1117.153046	−131.598	51.9622	8.7	6.5	36.7746

is observed in back-arc regions. The anisotropic patterns, however, are far more complex. A global compilation of mantle wedge anisotropy is provided by Long and Wirth (2013). In general, the subslab mantle is likely entrained by the subducting slab due to viscous coupling between them (Long & Silver, 2008), leading to a trench-normal fast-axis as well. In the subslab mantle, however, both trench-normal and trench-parallel fast directions have been observed in subduction settings (Lynner & Long, 2013, 2014; Roy et al., 2017); the former is often attributed to strong coupling between the down-going slab and the subslab asthenosphere, whereas the latter is caused by decoupling between them, which is likely promoted by slab rollback (Long & Silver, 2008). Long (2013) suggested that mantle flow in the mantle wedge and subslab mantle can be affected by many factors, such as the slab age, slab morphology, and surrounding flow field. Therefore, careful investigation of mantle anisotropy is essential for understanding which factors play the dominant role in controlling mantle dynamics in subduction zones.

5.2. Sources of Observed Seismic Anisotropy

In this study, core phase (*SKS*) splitting is used to characterize the seismic anisotropy, because using such a phase has two main advantages. First, this phase travels nearly vertically through the upper mantle, leading to a small incidence angle, which is important to minimize a distortion of waveform due to the strong interaction of the *S* wave with the free surface. Second, it is a *P*-to-*S* conversion phase at the core-mantle boundary (CMB), meaning that any observed splitting must be attributed to anisotropic layers on the receiver side between the surface and the CMB. However, *SKS* splitting has poor vertical resolution, leading to difficulty in interpreting the depth range of anisotropy. To constrain the depth distribution of anisotropy, we combine *SKS* splitting with other approaches such as local *S* and source-side *S* splitting (Figure 6), and then discuss the source of observed anisotropy from our *SKS* splitting results in the following sections.

5.3. Subslab Mantle Flow Caused by the Eastward Subduction of the Molucca Sea (Halmahera) Slab

The Molucca Sea plate is a micro-oceanic plate isolated from the larger Philippine Sea plate and became independent during westward subduction of the Pacific plate and northward drifting of the Indian-Austral-

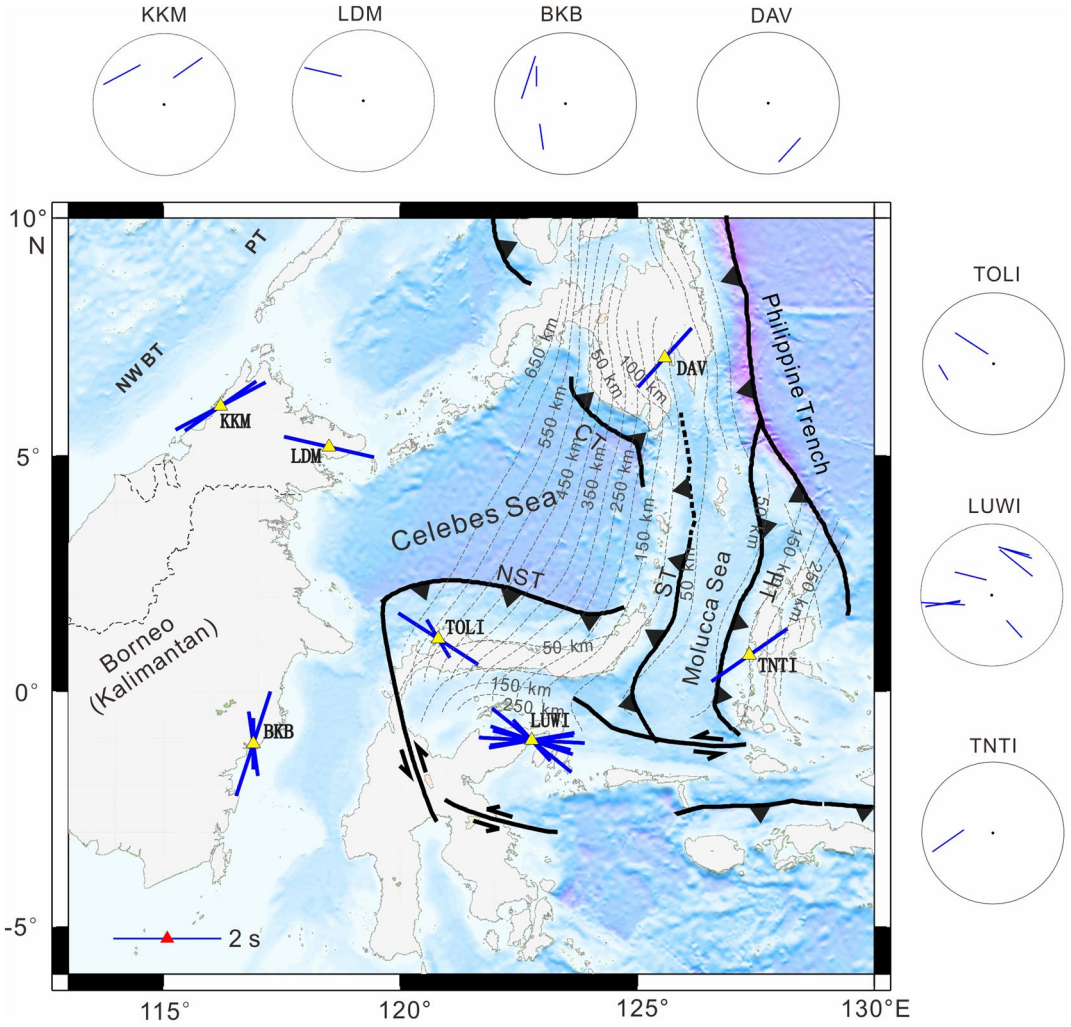

Figure 4. The results of all *SKS*-wave splitting measurements in this study. The orientation of each bar indicates the corresponding fast direction; the bar length is proportional to the delay time. The regional tectonic configuration is explained in Figure 1. The contour lines show depths to the upper boundaries of the subducting slabs with an interval of 50 km from Slab2 (Hayes et al., 2018). The surrounding seven circular diagrams show the lower hemisphere, equal-area projections of the splitting parameters at each station (as shown in yellow triangles in the map). Specifically, the outer circle represents an incidence angle of 15°. The orientation of each bar indicates the corresponding fast direction; the bar length is proportional to the delay time.

ian plate (R. Hall, 1996; Knesel et al., 2008). The formation and evolution of this area have been interpreted as consequences of both Pacific and Tethys tectonic processes, where the Molucca Sea plate is subducting westward at the Sangihe trench and eastward at the Halmahera trench with slab depths of ~650 and ~250 km, respectively (Cardwell et al., 1980; Hayes et al., 2018; Tatsumi et al., 1991). The Molucca Sea plate features an asymmetrical morphology as it descends into the upper mantle (Figure 7a). Several studies have been undertaken to shed light on mantle convection in this region (Di Leo et al., 2012a, 2012b; Roy et al., 2017). Di Leo et al. (2012a) carried out local *S* and *SKS*-wave splitting measurements at station MNI above the westward-subducting Sangihe slab and several source-side *S* phase splitting measurements from events beneath the Molucca Sea (Figure 6). They suggested that *SKS* fast directions at MNI are trench-parallel with one dominant horizontal layer of anisotropy. In addition, the average values of δt from splitting of *SKS* (1.53 s) and source-side *S* phases (1.33 s) are much larger than the average δt from splitting of local *S* (0.5 s), indicating (a) that the observed anisotropy from splitting of *SKS* and source-side *S* phases primarily originate from the subslab mantle, and (b) that the trench-parallel fast directions may reflect the CPO of olivine caused by mantle material squeezing outward to the north and south, which is likely due to

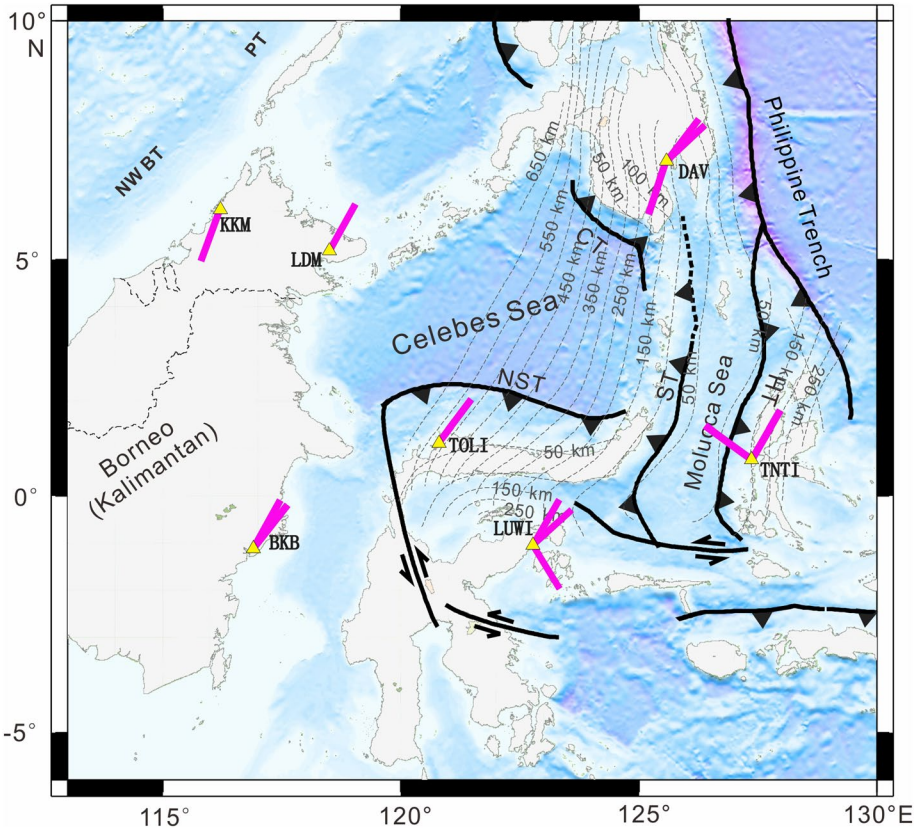

Figure 5. Null measurements at each station, which are plotted with a bar oriented along the back-azimuth. Other symbols are the same as those in Figure 4.

the double-sided subduction and rollback of the Molucca Sea slab (Di Leo et al., 2012a; Figures 7 and 8). Roy et al. (2017) also used source-side *S* phase splitting to characterize the subslab anisotropy beneath the Molucca Sea slab, and similar results were obtained.

In this study, we obtained a new splitting and two null measurements at station TNTI which offer new clues to understand the mantle flow pattern particularly associated with the eastward subduction of the Halmahera slab. The values of φ and δt at this station are constrained to 55° and 1.69 s, respectively. The fast direction appears to be inconsistent with the predictions from null measurement, probably indicating a more complex anisotropic structure in the upper mantle. This complication can be decoded by understanding what upper mantle structures are sampled by *SKS*-waves. The fact is that *SKS*-waves pass through the upper mantle, comprising the subslab mantle, subducting slab, mantle wedge and overlying lithosphere (Figure 7a). Although they propagate primarily through the subslab mantle, anisotropic structures above the slab likely contribute to the observed anisotropy, probably leading to a trench-oblique fast-axis. Note that TNTI is located in the forearc, in which the structures above a down-going slab primarily include the mantle wedge "nose" and the overriding crust (Figure 7a). The former has been growingly recognized to be isotropic due to its stagnant status (Uchida et al., 2020), whereas the latter's contribution to the anisotropy is also insignificant because the global average splitting time from the crust has been suggested to be on the order of 0.1 s (P. G. Silver, 1996). To make a conspicuous contribution to the observed anisotropy, another model is thus required. A thin layer of sheared hydrous material like serpentine has been suggested to situate directly above the slab, which may play an important role in producing the anisotropy (Olive et al., 2014; Wagner et al., 2013). Therefore, such a serpentine layer could contribute to the two-layer anisotropy, leading to a trench-oblique fast-axis observed at TNTI. The presence of two-layer anisotropic structure in the upper mantle might also explain the disagreement between the observed φ and null measurements. However, due to limited events, we are not able to characterize the anisotropy in each layer. Note that the subslab mantle may still serve as the main source of anisotropy, because a similar order of splitting time was observed at

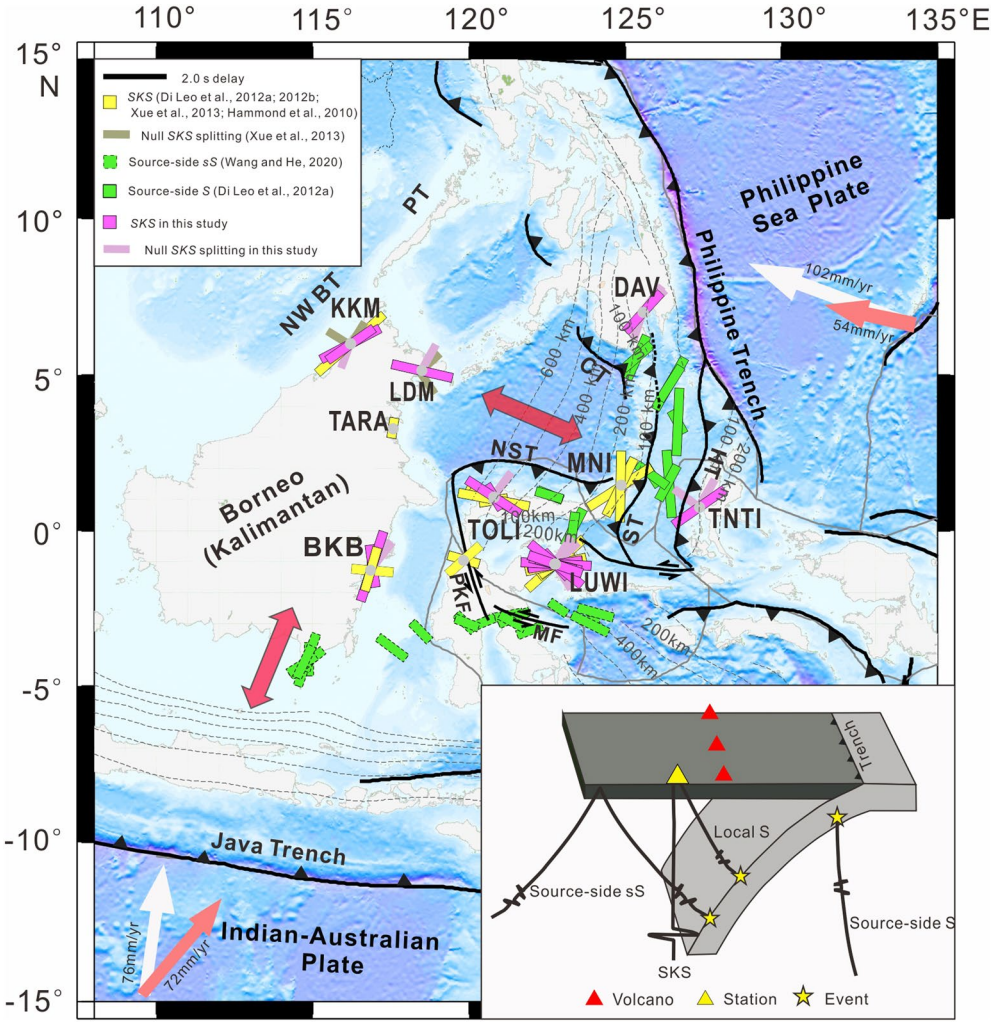

Figure 6. Comparison of average *SKS*-wave splitting observations in this study (purple bars) and previous splitting results. Bars are oriented in the fast direction and colored for different studies (yellow for the *SKS*-wave splitting measurements of Di Leo et al. (2012a, 2012b), Xue et al. (2013), and Hammond et al. (2010); green with dotted line for the source-side *sS*-wave splitting study by L. Wang and He (2020); green with solid line for the source-side *S*-wave splitting study by Di Leo et al. (2012a); gray and pink without a border for null *SKS*-wave results of Xue et al. (2013) and this study, respectively. Their lengths are proportional to delay times. Red arrows denote the expected corner flow direction induced by subduction of the Sangihe slab and the Indian-Australian slab. White and pink arrows indicate plate motion directions from two different absolute plate motion models: hotspot model by Gripp and Gordon (2002) and no-net-rotation model by DeMets et al. (1994). The inset cartoon illustrates raypaths of different shear waves.

MNI by Di Leo et al. (2012a), where the subslab mantle was suggested as the dominant source of observed seismic anisotropy (Figures 6 and 7a). In summary, all the observations consistently suggest the presence of a vigorous subslab mantle flow beneath the Molucca Sea, which plays the dominant role in governing the regional dynamics in the upper mantle.

5.4. Mantle Flow Above, Below, and Around the Westward-Subducting Molucca Sea (Sangihe) Slab

We conducted *SKS* splitting measurements at three stations, namely, TOLI, LUWI, and DAV. TOLI is situated above the westward-subducting Sangihe and southward subduction Celebes Sea slabs, and LUWI and DAV are located at the southern and northern edges of the Sangihe slab, respectively. Anisotropic results for these three stations can provide important clues to understanding regional mantle dynamics in the westward-subducting Sangihe subduction system.

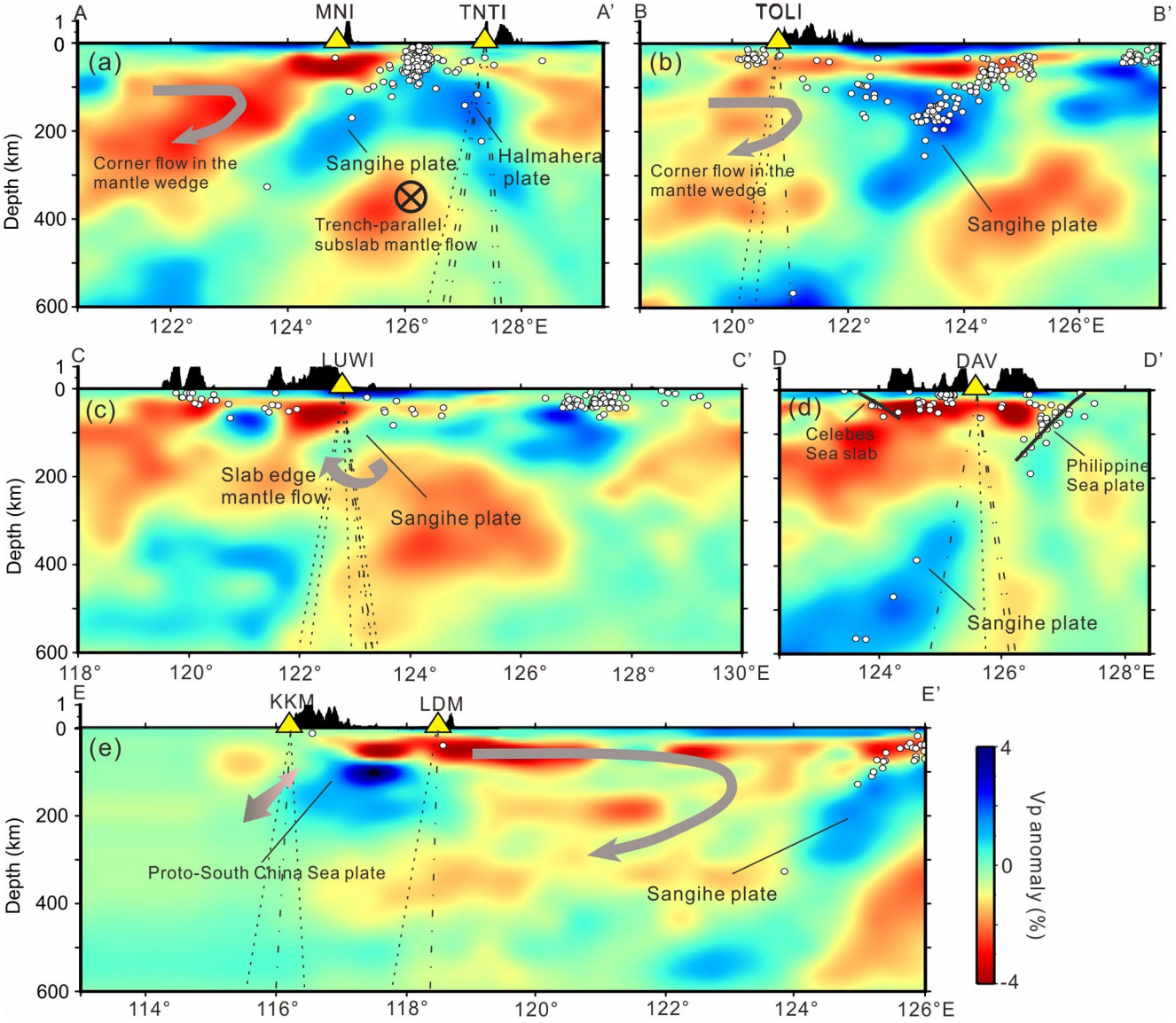

Figure 7. Interpretations of mantle flow patterns with the aid of *Vp* velocity perturbations in tomographic models by Amaru (2007). Mantle flow patterns along five vertical profiles (as shown in Figure 1) are presented. In general, the red and blue colors denote low and high *Vp* perturbations, respectively, whose scale is shown at the top right. White dots show earthquakes that occurred within a 20-km width along each profile. Yellow triangles represent stations used in this study shown in Figure 1 and station MNI from Di Leo et al. (2012b) shown in Figure 6. White dots show local seismicity spanning from 1990 to 2020 with magnitude >5 (the catalog is from USGS). Dotted lines delineate raypaths of *SKS* phases in the upper mantle defined by the source-receiver pairs. Topography is also depicted above each profile by the black areas. The gray bent arrows, and the circles with a cross and with a dot indicate the interpreted mantle flow patterns.

A NW–SE-trending fast-axis, oblique to the North Sulawesi trench and normal to the Sangihe trench, is observed at station TOLI, which is consistent with the previous results from Di Leo et al. (2012b), who suggested that the anisotropic fabrics are likely influenced by the subduction of both the Sangihe and Celebes Sea slabs. Here, three types of flow are likely to explain the observed anisotropy including: (a) mantle wedge flow above the subducting Celebes Sea slab, (b) subslab flow below the subducting Celebes Sea slab, and (c) mantle wedge flow above the subducting Sangihe slab. To help understand which type of flow may play the main role in governing the regional mantle dynamics, the upper mantle tomographic model UU-P07 given by Amaru (2007) is incorporated (Figure 7b). The seismicity within the subducting Celebes Sea slab along with the tomographic images clearly shows that the TOLI station lies ~60 km above the Celebes

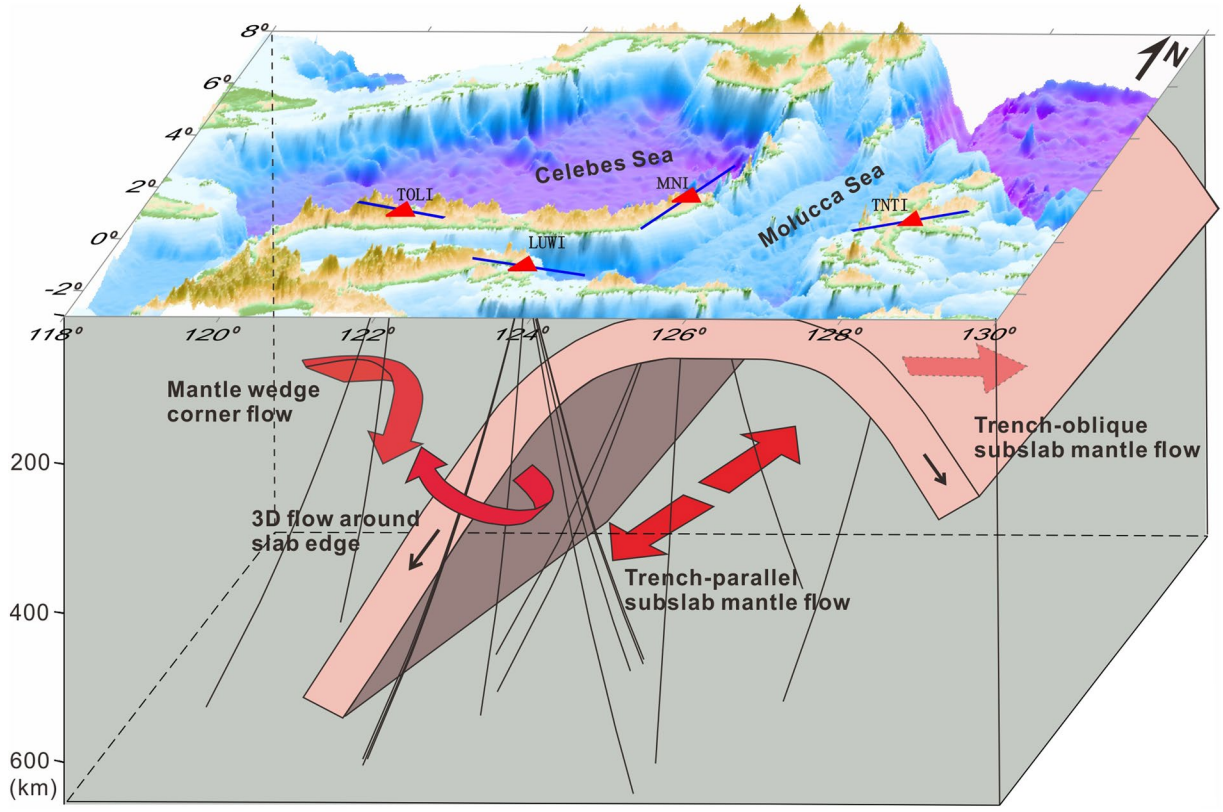

Figure 8. Cartoon illustrating various types of mantle flow (red arrows) above, below, and around the down-going Molucca Sea plate, which are interpreted according to the results from this study and Di Leo et al. (2012a). At the stations, the orientation of each solid thick bar indicates the average fast polarization direction at the station, and the bar length is proportional to the average delay time. The *SKS*-wave raypaths in the upper mantle are delineated with curved black lines.

Sea slab (Figure 7b), which is also suggested by the Slab2 model (Hayes et al., 2018) (Figure 6). Thus, the subducting Celebes Sea slab is thought to play a minor role in influencing corner flow within the mantle wedge due to its shallow subduction. This observation is consistent with several studies of mantle wedges beneath shallow subduction zones such as New Zealand (Morley et al., 2006) and Java-Sumatra (Hammond et al., 2010), which suggested that corner flow-induced deformation is not strong enough to develop coherent CPO in such a shallow mantle wedge. Note that the observed fast direction appears to be sub-parallel to the arcuate North Sulawesi trench, which may be explained by the subslab mantle flow facilitated by slab-mantle decoupling. However, the raypaths of *SKS* waves seemingly sample the subslab mantle marginally. The observed anisotropy may thus be partly influenced by the subslab mantle flow if a vigorous flow indeed takes place below the down-going Celebes Sea slab. In contrast, the Sangihe slab has reached a depth of 600 km or more, and a large mantle wedge has readily developed. Accordingly, corner flow is expected to occur in the large mantle wedge (Figure 7b), which is highly consistent with the observed trench-normal fast-axis with respect to the Sangihe trench at station TOLI. Therefore, we infer that the large mantle wedge flow associated with subduction of the Sangihe slab might contribute more to the observed anisotropy.

Station DAV is located in a region where multiple slabs are subducting. Specifically, the Philippine Sea and Celebes Sea plates are subducting westward and eastward, respectively, and both dip toward the center of the Mindanao Peninsula (Figure 7d; Amaru, 2007; Hayes et al., 2018). Meanwhile, the northern edge of the Sangihe slab reaches a depth of ~650 km beneath the northern region of Mindanao. The fast wave polarization direction (NE–SW) at DAV is consistent with the results by analyzing source-side *S*-wave splitting using the nearby events with depths between 30 and 50 km (green bars in Figure 6; Di Leo et al., 2012a). The delay time (1.44 s) observed here from *SKS* splitting is much larger than the average delay time of 0.37 s from local *S* splitting for events shallower than 200 km (Di Leo et al., 2012a), which imply that the mantle below

200 km depth must make a significant contribution to the observed anisotropy. The observed NE–SW fast direction is perhaps a result of interactions of dynamic processes associated with the three subducting slabs.

The fast directions observed here at LUWI are predominantly WNW–ESE-trending, which are different from the predominant NE–SW fast direction from four measurements detected by Di Leo et al. (2012b). The only same event on December 8, 2009 used in both studies has quite similar splitting results ($\varphi = 81°$ in this study and $\varphi = 77°$ by Di Leo et al., 2012b). In addition, our splitting results are also consistent with predictions of our null measurements. Therefore, the predominant fast-axis is most likely to be WNW–ESE-trending.

It is worthwhile to mention that LUWI is located near the southern edge of the subducting Sangihe slab, and numerical modeling has suggested that the mantle flow is deflected due to proximity to the edges of down-going slabs (Q. Zhang et al., 2017). Therefore, the edge effect must have a non-negligible influence on the observed anisotropy (Figures 7 and 8). A similar scenario due to the edge effect may also take place at DAV, because it is located near the northern edge of the subducting Sangihe slab.

5.5. Mantle Flow Beneath Eastern Borneo

Two stations KKM and LDM are located on northeastern Borneo. The fast direction at KKM is parallel to the Northwest Borneo-Palawan trough, whereas that at LDM is subnormal to the Northwest Borneo-Palawan trough. The *SKS* splitting measurements of Xue et al. (2013) show similar results at KKM but only null results at LDM. Our measurement at LDM provides the first splitting result, suggesting that the underlying mantle is not isotropic.

The observed fast wave polarization direction at LDM is oriented trench-normal with respect to the westward-subducting Sangihe slab, which has subducted as deep as ~650 km depth. This scenario can be explained by the existence of corner flow within the large mantle wedge developed by such a deep subduction, and development of a corner flow in the big mantle wedge with similar scale has been corroborated by numerical modeling (Dal Zilio et al., 2018). However, the direction observed at KKM is slightly different from that at LDM, which indicates that a dynamic process in the upper mantle has deflected the mantle flow. One possible mechanism is the presence of an extinct slab in the upper mantle because a high-velocity anomaly is observed in the upper mantle between KKM and LDM by tomographic imaging (Figure 7e; Amaru, 2007). Geological observations suggested that a paleoslab (the Proto-South China Sea slab) subducted beneath northern Borneo along the Northwest Borneo-Palawan trough (an extinct subduction trench) during the Paleogene (Hamilton, 1979). The subducted Proto-South China Sea plate has also been verified by the Cenozoic geological history of Borneo (R. Hall, 2013; Hutchison, 1996). Therefore, the subduction of the Proto-South China Sea plate played an important role in influencing the regional dynamics in the upper mantle beneath station KKM.

Station BKB is located on southwestern Borneo, and fast direction from three splitting results trends consistently NNE–SSW, which is normal to the Java trench. Previous *SKS*-wave splitting by Di Leo et al. (2012b) shows two splitting results at BKB: one is consistent with our results, but the other is quite different (Figure 6). Note that in this study, we not only present more measurements, but also present null measurements, and what is more important is that all our results are consistent. These fast directions are consistent with the results measured at nearby locations from source-side *sS* splitting by L. Wang and He (2020) (Figure 6), which reflects the mantle wedge corner flow in the back-arc region of the Java subduction zone. Again, like that observed at LDM, corner flow is recognized to play a very important role in influencing the regional dynamics in the mantle wedge.

6. Conclusion

The upper mantle deformation beneath the eastern Indonesian Archipelago has witnessed complex regional tectonic activity since the Mesozoic, with the northward drifting of the Indian-Australian plate and the westward subduction of the Pacific plate. By analyzing *SKS* splitting measurements at seven stations around the Celebes Sea at the junction of multiple subduction systems between the Pacific and Tethys domains, we present additional constraints on the dynamics in the regional upper mantle associated with interactions

among multiple microcontinents and oceanic plates. Combining our observations with previous results, we suggest that active, complex mantle flow patterns have taken place in the study area, including trench-normal corner flow caused by the westward-subducting Molucca Sea (Sangihe) slab, two-layer anisotropy related to the eastward-subducting Molucca Sea (Halmahera) slab, deflected mantle flow around the southern edge of the Sangihe slab, and mantle flow associated with the combined effects of multiple subducting slabs on the northern edges of the Sangihe slab. In addition, beneath northeastern Borneo, anisotropy signatures probably reflect mantle flow induced by the subducted Proto-South China Sea plate. Moreover, corner flow in the Java mantle wedge, which are induced by the subduction and rollback of the Indian-Australian plate, probable impact a broad region hundreds of kilometers away, even into southeastern Borneo.

Data Availability Statement

All waveforms in the horizontal components used in this study can be accessed from https://zenodo.org/record/4486193.

Acknowledgments
The manuscript benefits from constructive suggestions by Prof. Huaiyu Yuan. The authors are grateful to the thoughtful and constructive comments provided by two anonymous reviewers and the editors. Many thanks go to the Data Management Center of the Incorporated Research Institutions for Seismology (www.iris.edu) for providing the waveform data. The authors acknowledge support from the National Scientific Foundation of China (Grant Nos. 91858212, 42076068, 41730532, 91958212, and 91858205), the Strategic Priority Research Program of the Chinese Academy of Sciences (Grant No. XDB42020103), and Key Special Project for Introduced Talents Team of Southern Marine Science and Engineering Guangdong Laboratory (Guangzhou) (GML2019ZD0204). The Multiple Frequency Automatic Splitting Technique software can be obtained via http://mfast-package.geo.vuw.ac.nz/. Some figures were prepared using the Generic Mapping Tools (P. Wessel & Smith, 1991).

References

Amaru, M. L. (2007). *Global travel time tomography with 3-D reference models* (PhD thesis). Utrecht University.
Argus, D. F., Gordon, R. G., & DeMets, C. (2011). Geologically current motion of 56 plates relative to the no-net-rotation reference frame. *Geochemistry, Geophysics, Geosystems*, *12*, Q11001. https://doi.org/10.1029/2011GC003751
Aurelio, M. (1992). *Tectonique du segment central de la Faille Philippine: Étude structurale, cinématique et évolution géodynamique, thèse de doctorat* (p. 345). Université Pierre-et-Marie-Curie.
Bird, P. (2003). An updated digital model of plate boundaries. *Geochemistry, Geophysics, Geosystems*, *4*(3), 1027. https://doi.org/10.1029/2001GC000252
Bock, Y., Prawirodirdjo, L., Genrich, J. F., Stevens, C. W., McCaffrey, R., Subarya, C., et al. (2003). Crustal motion in Indonesia from Global Positioning System measurements. *Journal of Geophysical Research*, *108*, 2367. https://doi.org/10.1029/2001JB000324
Cardwell, R. K., Isacks, B. L., & Karig, D. E. (1980). The spatial distribution of earthquakes, focal mechanism solutions, and plate boundaries in the Philippine and Northeastern Indonesian Islands. In D. E. Hayes (Ed.), The tectonic and geologic evolution of southeast Asian seas and islands (Geophysical Monograph Series, Vol. 23, pp. 1–35). AGU. https://doi.org/10.1029/gm023p0001
Christensen, N. I. (1984). The magnitude, symmetry and origin of upper mantle anisotropy based on fabric analyses of ultramafic tectonites. *Geophysical Journal of the Royal Astronomical Society*, *76*, 89–111. https://doi.org/10.1111/j.1365-246x.1984.tb05025.x
Cottam, M. A., Hall, R., Forster, M., & Boudagher Fadel, M. (2011). Basement character and basin formation in Gorontalo Bay, Sulawesi, Indonesia: New observations from the Togian Islands. In R. Hall, M. A. Cottam, & M. E. J. Wilson (Eds.), The SE Asian gateway: History and tectonics of Australia–Asia collision (Vol. 355, pp. 177–202). Geological Society of London Special Publication. https://doi.org/10.1144/sp355.9
Dal Zilio, L., Faccenda, M., & Capitanio, F. (2018). The role of deep subduction in super-continent breakup. *Tectonophysics*, *746*, 312–324. https://doi.org/10.1016/j.tecto.2017.03.006
DeMets, C., Gordon, R. G., & Argus, D. F. (2010). Geologically current plate motions. *Geophysical Journal International*, *181*, 1–80. https://doi.org/10.1111/j.1365-246x.2009.04491.x
DeMets, C., Gordon, R. G., Argus, D. F., & Stein, S. (1994). Effect of recent revisions to the geomagnetic reversal time scale on estimates of current plate motions. *Geophysical Research Letters*, *21*(20), 2191–2194. https://doi.org/10.1029/94GL02118
Di Leo, J. F., Wookey, J., Hammond, J. O. S., Kendall, J. M., Kaneshima, S., Inoue, H., et al. (2012a). Deformation and mantle flow beneath the Sangihe subduction zone from seismic anisotropy. *Physics of the Earth and Planetary Interiors*, *194–195*(C), 38–54. https://doi.org/10.1016/j.pepi.2012.01.008
Di Leo, J. F., Wookey, J., Hammond, J. O. S., Kendall, J. M., Kaneshima, S., Inoue, H., et al. (2012b). Mantle flow in regions of complex tectonics: Insights from Indonesia. *Geochemistry, Geophysics, Geosystems*, *13*, Q12008. https://doi.org/10.1029/2012GC004417
Elburg, M., & Foden, J. (1998). Temporal changes in arc magma geochemistry, northern Sulawesi, Indonesia. *Earth and Planetary Science Letters*, *163*, 381–398. https://doi.org/10.1016/s0012-821x(98)00143-5
Engdahl, E. R., Di Giacomo, D., Sakarya, B., Gkarlaouni, C. G., Harris, J., & Storchak, D. A. (2020). ISC-EHB 1964-2016, an improved data set for studies of Earth structure and global seismicity. *Earth and Space Science*, *7*(1), e2019EA000897. https://doi.org/10.1029/2019EA000897
Engdahl, E. R., & Gunst, R. H. (1966). Use of a high speed computer for the preliminary determination of earthquake hypocenters. *Bulletin of the Seismological Society of America*, *56*, 325–336. https://doi.org/10.1785/bssa0560020325
Fan, J., & Zhao, D. (2019). P-wave anisotropic tomography of the central and southern Philippines. *Physics of the Earth and Planetary Interiors*, *286*, 154–164. https://doi.org/10.1016/j.pepi.2018.12.001
Fan, J., Zhao, D., Dong, D., & Zhang, G. (2017). P-wave tomography of subduction zones around the central Philippines and its geodynamic implications. *Journal of Asian Earth Sciences*, *146*, 76–89. https://doi.org/10.1016/j.jseaes.2017.05.015
Fang, N. Q. (2002). Major features of the sedimentary records from the Indonesian Archipelago and research on the Paleo-Tethys in Yunnan. *Earth Science Frontiers*, *9*(3), 173–181. (in Chinese with English abstract)
Gripp, A. E., & Gordon, R. G. (2002). Young tracks of hotspots and current plate velocities. *Geophysical Journal International*, *150*(2), 321–361. https://doi.org/10.1046/j.1365-246X.2002.01627.x
Hall, C. E., Fischer, K. M., Parmentier, E. M., & Blackman, D. K. (2000). The influence of plate motions on three-dimensional back arc mantle flow and shear wave. *Journal of Geophysical Research*, *105*(B12), 28009–28033. https://doi.org/10.1029/2000jb900297
Hall, R. (1996). Reconstructing Cenozoic SE Asia. *Geological Society, London, Special Publications*, *106*, 153–184. https://doi.org/10.1144/gsl.sp.1996.106.01.11

Hall, R. (2012). Late Jurassic–Cenozoic reconstructions of the Indonesian region and the Indian Ocean. *Tectonophysics*, *570–571*, 1–41. https://doi.org/10.1016/j.tecto.2012.04.021
Hall, R. (2013). Contraction and extension in Northern Borneo driven by subduction rollback. *Journal of Asian Earth Sciences*, *76*, 399–411. https://doi.org/10.1016/j.jseaes.2013.04.010
Hall, R. (2017). SE Asia: New views of the geology of the Malay Archipelago. *Annual Review of Earth and Planetary Sciences*, *45*, 331–358. https://doi.org/10.1146/annurev-earth-063016-020633
Hall, R., & Sevastjanova, I. (2012). Australian crust in Indonesia. *Australian Journal of Earth Sciences*, *59*, 827–844. https://doi.org/10.1080/08120099.2012.692335
Hall, R., & Spakman, W. (2015). Mantle structure and tectonic history of SE Asia. *Tectonophysics*, *658*(C), 14–45. https://doi.org/10.1016/j.tecto.2015.07.003
Hall, R., van Hattum, M. W. A., & Spakman, W. (2008). Impact of India–Asia collision on SE Asia: The record in Borneo. *Tectonophysics*, *451*, 366–389. https://doi.org/10.1016/j.tecto.2007.11.058
Hall, R., & Wilson, M. E. J. (2000). Neogene sutures in eastern Indonesia. *Journal of Asian Earth Sciences*, *18*, 787–814. https://doi.org/10.1016/s1367-9120(00)00040-7
Hamilton, W. (1979). *Tectonics of the Indonesian region 1078* (p. 345). U.S. Geological Survey Professional Paper.
Hammond, J. O. S., Wookey, J., Kaneshima, S., Inoue, H., Yamashina, T., & Harjadi, P. (2010). Systematic variation in anisotropy beneath the mantle wedge in the Java-Sumatra subduction system from shear-wave splitting. *Physics of the Earth and Planetary Interiors*, *178*, 189–201. https://doi.org/10.1016/j.pepi.2009.10.003
Hayes, G. P., Moore, G. L., Portner, D. E., Hearne, M., Flamme, H., Furtney, M., & Smoczyk, G. M. (2018). Slab2, a comprehensive subduction zone geometry model. *Science*, *88*, 61. https://doi.org/10.1126/science.aat4723
Hess, H. (1964). Seismic anisotropy of the uppermost mantle under Oceans. *Nature*, *203*, 629–631. https://doi.org/10.1038/203629a0
Hutchinson, C. S. (2006). The Rajang accretionary prism and Lupar Line problem of Borneo. In R. Hall, & D. J. Blundell (Eds.), *Tectonic evolution of SE Asia* (Vol. 106, pp. 247–261). Geological Society, London, Special Publications.
Hutchison, C. S. (1996). The 'Rajang accretionary prism' and 'Lupar Line' problem of Borneo. In R. Hall, & D. J. Blundell (Eds.), *Tectonic evolution of southeast Asia* (Vol. 106, pp. 247–261). Geological Society, London, Special Publications. https://doi.org/10.1144/gsl.sp.1996.106.01.16
Jaffe, L. A., Hilton, D. R., Fischer, T. P., & Hartono, U. (2004). Tracing magma sources in an arc–arc collision zone: Helium and carbon isotope and relative abundance systematics of the Sangihe Arc, Indonesia. *Geochemistry, Geophysics, Geosystems*, *5*, Q04J10. https://doi.org/10.1029/2003GC000660
Király, Á., Capitanio, F. A., Funiciello, F., & Faccenna, C. (2016). Subduction zone interaction: Controls on arcuate belts. *Geology*, *44*(9), 715–718. https://doi.org/10.1130/G37912.1
Király, Á., Holt, A. F., Funiciello, F., Faccenna, C., & Capitanio, F. A. (2018). Modeling slab-slab interactions: Dynamics of outward dipping double-sided subduction systems. *Geochemistry, Geophysics, Geosystems*, *110*, 693–714. https://doi.org/10.1002/2017GC007199
Knesel, K. M., Cohen, B. E., Vasconcelos, P. M., & Thiede, D. S. (2008). Rapid change in drift of the Australian plate records collision with Ontong Java plateau. *Nature*, *454*(7205), 754–757. https://doi.org/10.1038/nature07138
Kopp, C., Flueh, E. R., & Neben, S. (1999). Rupture and accretion of the Celebes Sea crust related to the North-Sulawesi subduction: Combined interpretation of reflection and refraction seismic measurements. *Geodynamics*, *27*, 309–325. https://doi.org/10.1016/s0264-3707(98)00004-0
Lallemand, S. E., Popoff, M., Cadet, J.-P., Bader, A.-G., Pubellier, M., Rangin, C., & Deffontaines, B. (1998). Genetic relations between the central and southern Philippine trench and the Sangihe trench. *Journal of Geophysical Research*, *103*(B1), 933–950. https://doi.org/10.1029/97jb02620
Liu, B. P., Feng, Q. L., & Fang, N. Q. (1991). Tectonic evolution of the Paleo-Tethys in Changning-Menglian Belt and adjacent region, western China. *Journal of China University of Geosciences*, *2*, 18–28. (in Chinese with English abstract)
Liu, C., & Shi, Y. L. (2021). Space-time stress variations on the Palu-Koro fault impacting the 2018 Mw 7.5 Palu earthquake and its seismic hazards. *Geochemistry, Geophysics, Geosystems*. https://doi.org/10.1029/2020GC009552
Long, M. D. (2013). Constrains on subduction geodynamics from seismic anisotropy. *Reviews of Geophysics*, *51*, 76–112. https://doi.org/10.1002/rog.20008
Long, M. D., & Silver, P. G. (2008). The subduction zone flow field from seismic anisotropy: A global view. *Science*, *319*(5861), 315–318. https://doi.org/10.1126/science.1150809
Long, M. D., & Wirth, E. A. (2013). Mantle flow in subduction systems: The mantle wedge flow field and implications for wedge processes. *Journal of Geophysical Research: Solid Earth*, *118*, 583–606. https://doi.org/10.1002/jgrb.50063
Lynner, C., & Long, M. D. (2013). Sub-slab seismic anisotropy and mantle flow beneath the Caribbean and Scotia subduction zones: Effects of slab morphology and kinematics. *Earth and Planetary Science Letters*, *361*, 367–378. https://doi.org/10.1016/j.epsl.2012.11.007
Lynner, C., & Long, M. D. (2014). Sub-slab anisotropy beneath the Sumatra and circum-Pacific subduction zones from source-side shear wave splitting observations. *Geochemistry, Geophysics, Geosystems*, *15*, 2262–2281. https://doi.org/10.1002/2014GC005239
Lyu, T., Zhu, Z., & Wu, B. (2019). Subducting slab morphology and mantle transition zone upwelling in double-slab subduction models with inward-dipping directions. *Geophysical Journal International*, *218*(3), 2089–2105. https://doi.org/10.1093/gji/ggz268
Morley, A. M., Stuart, G. W., Kendall, J.-M., & Reyners, M. (2006). Mantle wedge anisotropy in the Hikurangi subduction zone, Central North Island, New Zealand. *Geophysical Research Letters*, *33*. https://doi.org/10.1029/2005GL024569
Nicolas, A., & Christensen, N. I. (1987). Formation of anisotropy in upper mantle peridotites—A review. In K. Fuchs, & C. Froidevaux (Eds.), *Composition, structure and dynamics of the lithosphere-asthenosphere system* (pp. 111–123). https://doi.org/10.1029/GD016p0111
Nuttli, O. W. (1961). The effect of the earth's surface on the S-wave particle motion. *Bulletin of the Seismological Society of America*, *51*, 237–246. https://doi.org/10.1785/bssa0510020237
Olive, J.-A., Pearce, F., Rondenay, S., & Behn, M. D. (2014). Pronounced zonation of seismic anisotropy in the Western Hellenic subduction zone and its geodynamic significance. *Earth and Planetary Science Letters*, *391*, 100–109. https://doi.org/10.1016/j.epsl.2014.01.029
Parkinson, C. D., Miyazaki, K., Wakita, K., Barber, A. J., & Carswell, D. A. (1998). An overview and tectonic synthesis of the pre-Tertiary very high-pressure metamorphic and associated rocks of Java, Sulawesi and Kalimantan, Indonesia. *Island Arc*, *7*, 184–200. https://doi.org/10.1046/j.1440-1738.1998.00184.x
Ribe, N. M. (1989). Seismic anisotropy and mantle flow. *Journal of Geophysical Research*, *94*(B4), 4213–4223. https://doi.org/10.1029/jb094ib04p04213
Roy, S. K., Ravi Kumar, M., & Davuluri, S. (2017). Anisotropy in subduction zones: Insights from new source side S-wave splitting measurements from India. *Journal of Geophysical Research: Solid Earth*, *115*, 6454–6472. https://doi.org/10.1002/2017JB014314

Sajona, F. G., Bellon, H., Maurg, R., Pubellier, M., Quebral, R. D., Cotton, J., et al. (1997). Tertiary and Quaternary magmatism in Mindanao and Leyte (Philippines): Geochronology, geochemistry and tectonic setting. *Journal of Asian Earth Sciences*, *15*(2–3), 121–153. https://doi.org/10.1016/s0743-9547(97)00002-0

Savage, M. K., Wessel, A., Teanby, N., & Hurst, T. (2010). Automatic measurement of shear wave splitting and applications to time varying anisotropy at Mt. Ruapehu volcano, New Zealand. *Journal of Geophysical Research*, *115*, B12321. https://doi.org/10.1029/2010JB007722

Silver, E. A., & Moore, J. C. (1978). The Molucca Sea collision zone, Indonesia. *Journal of Geophysical Research*, *83*, 1681–1691. https://doi.org/10.1029/jb083ib04p01681

Silver, P. G. (1996). Seismic anisotropy beneath the continents: Probing the depths of geology. *Annual Review of Earth and Planetary Sciences*, *24*, 385–432. https://doi.org/10.1146/annurev.earth.24.1.385

Silver, P. G., & Savage, M. K. (1994). The interpretation of shear wave splitting parameters in the presence of two anisotropic layers. *Geophysical Journal International*, *119*, 949–963. https://doi.org/10.1111/j.1365-246x.1994.tb04027.x

Simons, W. J. F., Socquet, A., Vigny, C., Ambrosius, B. A. C., Abu, S. H., Promthong, C., et al. (2007). A decade of GPS in Southeast Asia: Resolving Sundaland motion and boundaries. *Journal of Geophysical Research*, *112*, B06420. https://doi.org/10.1029/2005JB003868

Tatsumi, Y., Murasaki, M., Arsadi, E. M., & Nohda, S. (1991). Geochemistry of Quaternary lavas from NE Sulawesi: Transfer of subduction components into the mantle wedge. *Contributions to Mineralogy and Petrology*, *107*, 137–149. https://doi.org/10.1007/bf00310703

Teanby, N., Kendall, J. M., & Van der Baan, M. (2004). Automation of shear-wave splitting measurements using cluster analysis. *Bulletin of the Seismological Society of America*, *94*(2), 453–463. https://doi.org/10.1785/0120030123

Uchida, N., Nakajima, J., Wang, K., Takagi, R., Yoshida, K., Nakayama, T., et al. (2020). Stagnant forearc mantle wedge inferred from mapping of shear-wave anisotropy using S-net seafloor seismometers. *Nature Communications*, *11*(1), 5676. https://doi.org/10.1038/s41467-020-19541-y

van Leeuwen, T. M., Allen, C. M., Kadarusman, A., Elburg, M., Palin, J. M., Muhardjo, & Suwijianto (2007). Petrologic, isotopic, and radiometric age constraints on the origin and tectonic history of the Malino Metamorphic Complex, NW Sulawesi, Indonesia. *Journal of Asian Earth Sciences*, *29*, 751–777. https://doi.org/10.1016/j.jseaes.2006.05.002

Wagner, L. S., Fouch, M. J., James, D. E., & Long, M. D. (2013). The role of hydrous phases in the formation of trench parallel anisotropy: Evidence from Rayleigh waves in Cascadia. *Geophysical Research Letters*, *40*(11), 2642–2646. https://doi.org/10.1002/grl.50525

Wakita, K., Sopaheluwakan, J., Miyazaki, K., Zulkarnain, I., & Munasri, M. (1996). Tectonic evolution of the Bantimala Complex, South Sulawesi, Indonesia. *Geological Society, London, Special Publications*, *106*, 353–364. https://doi.org/10.1144/gsl.sp.1996.106.01.23

Wan, B., Wu, F., Chen, L., Zhao, L., Liang, X., Xiao, W., & Zhu, R. (2019). Cyclical one-way continental rupture-drift in the Tethyan evolution: Subduction-driven plate tectonics. *Science China Earth Sciences*, *62*, 2005–2016. https://doi.org/10.1007/s11430-019-9393-4

Wang, L., & He, X. (2020). Seismic anisotropy in the Java-Banda and Philippine subduction zones and its implications for the mantle flow system beneath the Sunda Plate. *Geochemistry, Geophysics, Geosystems*, *21*, e2019GC008658. https://doi.org/10.1029/2019GC008658

Wang, X., Kaus, B. J. P., Zhao, L., Yang, J., & Li, Y. (2019). Mountain building in Taiwan insights from 3-D geodynamic models. *Journal of Geophysical Research: Solid Earth*, *124*, 7588–7603. https://doi.org/10.1029/2018jb017165

Wessel, A. (2010). *Automatic shear wave splitting measurements at Mt. Ruapehu volcano, New Zealand* (Master's thesis). Victoria University of Wellington.

Wessel, P., & Smith, W. H. F. (1991). Free software helps map and display data. *Eos, Transactions American Geophysical Union*, *72*(41), 441–441. https://doi.org/10.1029/90EO00319

Wolfe, C. J., & Silver, P. G. (1998). Seismic anisotropy of oceanic upper mantle: Shear wave splitting methodologies and observations. *Journal of Geophysical Research*, *103*, 749–771. https://doi.org/10.1029/97jb02023

Xue, M., Le, K. P., & Yang, T. (2013). Seismic anisotropy surrounding South China Sea and its geodynamic implications. *Marine Geophysical Researches*, *34*, 407–429. https://doi.org/10.1007/s11001-013-9194-4

Zhang, Q., Guo, F., Zhao, L., & Wu, Y. (2017). Geodynamics of divergent double subduction: 3-D numerical modeling of a Cenozoic example in the Molucca Sea region, Indonesia. *Journal of Geophysical Research: Solid Earth*, *122*, 3977–3998. https://doi.org/10.1002/2017JB013991

Zhang, S., & Karato, S. (1995). Lattice preferred orientation of olivine aggregates deformed in simple shear. *Nature*, *375*, 774–777. https://doi.org/10.1038/375774a0